

# Copolymeric Network Crown Ether Resins with Pendent Functional Group: Synthesis and Adsorption for Metal Ions

LINGZHI MENG, LING HU, YUANYIN CHEN, CHUANQING DU, YOUWEI WANG

Department of Chemistry, Wuhan University, Wuhan, 430072, People's Republic of China

Received 11 May 1999; accepted 18 May 1999

**ABSTRACT:** Three network crown ether resins with a high content of pendent functional groups were prepared and characterized by IR, elemental analysis, and thermal analysis. The slight variance of the thermal stability of the resins was related to the kind and content of the pendent functional group. The adsorption capacity of the resins for Mg(II), Cu(II), Co(II), Pb(II), and Hg(II) was determined. Toward Hg(II), the adsorption capacity of the resins was high and the adsorption process was easy and spontaneously performed. The XPS study showed that the adsorption of the NCR–SN resin toward Cu(II), Pb(II), and Hg(II) was mainly the coordinate interactions between the ligand atom (S, N) of the pendent functional groups and the metal ions. © 2000 John Wiley & Sons, Inc. *J Appl Polym Sci* 76: 1457–1465, 2000

**Key words:** adsorption; copolymerization; network crown ether; crown ether resin

## INTRODUCTION

It is well known that crown ether polymers possess a number of merits as compared with monomeric crown ethers in the ease of separation and recovery from reaction systems as well as the reusability in the following runs. Several macrocyclic polyethers and azacrown ethers attached to polymer supports have been prepared and successfully used as exchangers and adsorbents.<sup>1–4</sup> However, their applications are very limited due to multiple-step synthetic procedures, which usually use monomeric crown ethers as starting materials. Therefore, it was a goal in this field to employ a more convenient method to prepare crown ether polymers from noncrown ether monomers. Warshawsky et al.<sup>5</sup> prepared polymers of pseudocrown ethers from the reaction of chloromethylated polystyrene with the sodium salt of poly(ethylene glycol). These pseudocrown ethers

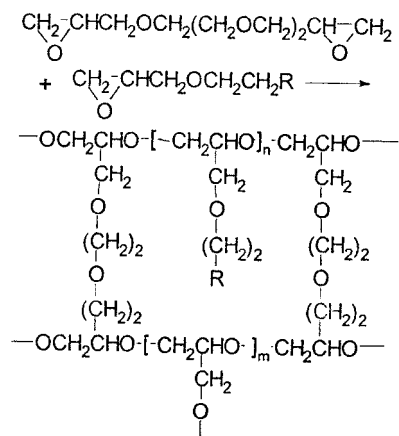
can efficiently complex transition-metal ions instead of alkali metal and alkali-earth metal ions, due to the bigger ring of the pseudocrown ether. Polymeric pseudocrown ether resins containing azacrown ether and azathiocrown ether were also reported.<sup>6</sup> These resins possess high selectivity for the adsorption of platinum group metal ions.

In this field, we also found a route to synthesize network crown ether polymers from noncrown ether monomers.<sup>7</sup> We first reported on network crown ether polymers with pendent functional groups in 1990.<sup>8</sup> But in the polymers [i.e., copolymerization of polyethylene glycol bisglycidyl ether with glycidyl ether substituted by quaternary ammonium salt], the amount of the pendent centric functional group was very low and the nitrogen content of the polymers was only about 0.1%. This article reports on a modified route for the synthesis of network crown ether resins with a higher content of pendent functional groups. The reaction route and possible structures of the copolymeric network crown ether resins (NCR) are shown in Scheme 1. These copolymers with a high content of pendent functional groups can efficiently adsorb the divalent mercury ion.

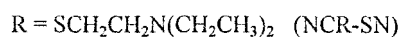
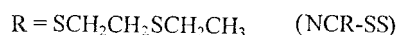
Correspondence to: Y. Chen.

Contract grant sponsor: National Nature Science Foundation of China.

*Journal of Applied Polymer Science*, Vol. 76, 1457–1465 (2000)  
© 2000 John Wiley & Sons, Inc.



$$n, m = 0, 1, 2, \dots$$



**Scheme 1**

## EXPERIMENTAL

### Materials

1-Chloro-2,3-epoxypropane was purified by distillation before use. Diethylene glycol bisglycidyl ether was prepared according to the literature.<sup>9</sup> 3-Thiopentyl alcohol was prepared by the reaction of  $\beta$ -mercaptoethyl alcohol with ethyl bromide in the presence of sodium methylate in absolute methanol; yield: 70%; bp 84°C (2.0 kPa); literature (ref. 10), 90°C (3.33 kPa). 3,6-Dithiooctyl alcohol was prepared by the reaction of  $\beta$ -mercaptoethyl alcohol with 3-thiopentyl chloride in the presence of sodium methylate in absolute methanol<sup>11</sup>; yield: 95%; bp 149°C (0.67 kPa). 5-Diethylamino-3-thiopentyl alcohol was prepared by the reaction of  $\beta$ -chloroethyl diethylamine hydrochloride with  $\beta$ -mercaptoethyl alcohol in the presence of sodium methylate in methanol; yield: 80%; bp 94–95°C (0.2 kPa), literature (ref. 12), 91.2°C (0.19 kPa). Butyl lithium was prepared using butyl chloride with metal lithium in cyclohexane dried by metal sodium. Other reagents were supplied by Shanghai Chemical Reagents Co. (Shanghai, China). They are laboratory-grade chemicals.

### Measurements

Elemental analysis was done on a 1106 elemental autoanalysis apparatus (Carlo-Erba, Italy). The

IR spectra were recorded on a Nicolet 170SX FTIR spectrometer. <sup>1</sup>H-NMR spectra were obtained on an EM-360L spectrometer (Varian, USA). The TG and DSC were carried out on an STA 409C thermal analyzer (Netzsch, German). The runs were performed at a heating rate of 20°C/min from 40 to 700°C in an atmosphere of dry nitrogen (100 mL/min). XPS was done on a Kratos XSAM 800 electron energy spectrometer. The concentrations of the metal ions were determined by titration or by a 180-80 atomic absorption spectrometer (AAS, Hitachi, Japan).

### Preparation of Substituted Glycidyl Ethers

3-Thiopentyl alcohol (5.3 g, 0.05 mol), 15 mL of dichloromethane, PEG-400 (1 g), and potassium hydroxide (2.8 g, 0.05 mol) were added to a 100-mL round flask equipped with a magnetic stirrer. Then, epichlorohydrin (9.25 g, 0.1 mol) was dropped into the flask and stirred at 35°C for 12 h. After filtration, the filtrate was distilled under reduced pressure. 3-Thiopentyl glycidyl ether (6 g, GE-S) was obtained as a colorless liquid; yield: 74%; bp 78°C (0.08 kPa).

3,6-Dithiooctyl glycidyl ether (GE-SS) or 5-diethylamino-3-thiopentyl glycidyl ether (GE-SN) was prepared similarly by using 3,6-dithiooctyl alcohol or 5-diethylamino-3-thiopentyl alcohol, respectively. The yield of GE-SS was 70.3%; bp 128–130°C (0.02 kPa), colorless liquid. The yield of GE-SN was 60.0%; bp 126–128°C (6.7 Pa), colorless liquid. The structure characterizations of the three substituted glycidyl ethers are listed in Table I.

### Preparation of NCR Resins

The NCR-S resin was prepared by ring-opening copolymerization of diethylene glycol bisglycidyl ether and GE-S. A mixture of diethylene glycol bisglycidyl ether (1.795 g, 8.23 mmol), GE-S (1.335 g (8.23 mmol), diethylene glycol (48.2 mg, 0.46 mmol), and sodium (14.2 mg, 0.62 mmol) was stirred at room temperature for 0.5 h under a nitrogen atmosphere and then at 120°C for 2.5 h. The reactants turned into a brown transparent solid after cooling. The solid was ground to powder and washed with distilled water until the filtrate remained neutral. Then, the copolymer was extracted by acetone for 12 h and dried at 120°C under reduced pressure to a constant weight. NCR-S, 2.52 g, was obtained as a light yellow powder; yield: 80.5%.

The NCR-SS resin and the NCR-SN resin were prepared similarly by using GE-SS or

**Table I Analysis of Alkyl Glycidyl Ethers**

GE-S	S 19.75 (19.70); MS: 162 (3.5) M <sup>+</sup> , 89 (100) C <sub>2</sub> H <sub>5</sub> SC <sub>2</sub> H <sub>4</sub> <sup>+</sup> ; <sup>1</sup> H-NMR: 1.18 (t 3H), 2.3–2.8 (m 6H), 2.8–3.2 (m 1H), 3.3–3.8 (m 4H). IR: 1460, 1270, 916, 860, 770 cm <sup>-1</sup>
GE-SS	S 28.79 (28.82); MS: 222 (7.5) M <sup>+</sup> 122 (52) C <sub>2</sub> H <sub>5</sub> SC <sub>2</sub> H <sub>4</sub> SH <sup>+</sup> ; <sup>1</sup> H-NMR: 1.18 (t 3H), 2.3–2.8 (m 10H), 2.8–3.2 (m 1H), 3.3–3.8 (m 4H). IR: 1462, 1274, 916, 860, 770 cm <sup>-1</sup>
GE-SN	S 13.68 (13.73), N 5.98 (6.00); MS: 233 (3.2) M <sup>+</sup> 86 (100) (C <sub>2</sub> H <sub>5</sub> ) <sub>2</sub> NC <sub>2</sub> H <sub>4</sub> <sup>+</sup> ; <sup>1</sup> H-NMR: 1.02 (t 6H), 2.2–2.8 (m 12H), 2.8–3.2 (m 1H), 3.2–3.9 (m 4H). IR: 1465, 1255, 915, 860, 700 cm <sup>-1</sup>

Elemental analysis (% Calcd); MS (*m/z*, RI); <sup>1</sup>H-NMR (CDCl<sub>3</sub>, δ ppm) and IR (cm<sup>-1</sup>).

GE-SN instead of GE-S; yield: 96.1 and 83.8%, respectively. The analysis and characterization of three copolymeric network crown ether resins are shown in Table II and Figures 1 and 2.

#### Adsorption of Resin for Metal Ions<sup>13</sup>

Twenty milligrams (*W*) of the resin and 10 mL (*V*) of the metal ion solution of a known concentration (*C<sub>i</sub>*) were placed in a 25-mL closed flask. A series of such flasks was shaken at a constant speed (150 times/min) and at a specified constant temperature for 2 h. The adsorption equilibrium was reached after 2 h. The metal ion concentration (*C<sub>e</sub>*) of the liquid phase was determined by titration with EDTA for Hg(II), Cu(II), and Pb(II) and by AAS for other metal ions. The adsorption capacity (*Q*) was calculated as follows:

$$Q = (C_i - C_e)V/W \text{ (mmol/g)}$$

## RESULTS AND DISCUSSION

#### The Monomeric Unit Ratio in the Copolymer

The monomeric unit ratio in the copolymer was calculated by the content of sulfur or nitrogen given by Table II. The ratio of diethylene glycol bisglycidyl ether to substituted glycidyl ether was

1:0.672, 1:1.037, and 1:0.684 for NCR-S, NCR-SS, and NCR-SN, respectively. The results showed that the copolymer with a high content of pendent functional groups can be prepared efficiently by the modified route.

#### IR Analysis

The IR spectra of NCR-S, NCR-SS, and NCR-SN were measured and are shown in Figure 1 (1600–400cm<sup>-1</sup>). Figure 1 shows that the adsorption bands of the epoxy group (about 916 and 860 cm<sup>-1</sup>) disappear; νC—S, δCH<sub>2</sub>—S, δCH<sub>2</sub>, and νC—O are around 660 (w), 1260, 1460, and 1110 cm<sup>-1</sup>, respectively. νC—N was covered by the width band of the C—O stretching vibration. Compared with substituted glycidyl ether, νC—S moves to a lower wavenumber. It can be attributed to the pendent functional groups and the effect of the network unit in the copolymer.

#### Thermal Analysis<sup>14</sup>

Thermal analysis curves of NCR-S, NCR-SS, and NCR-SN are presented in Figures 2(a–c), respectively. TG curves of NCR-S, NCR-SS, and NCR-SN did not show a decrease in the sample weight until 350, 220, and 280°C, respectively. It was found that the weight loss of three resins was less than 10, 50, and 80% at 320, 370, and 400°C,

**Table II Elemental Analysis of Resins (% Calcd)**

Resin	C	H	S	N
NCR-S	53.4 (53.7)	8.6 (8.5)	5.66 (8.43)	—
NCR-SS	51.9 (51.8)	8.0 (8.2)	15.09 (14.55)	—
NCR-SN	55.5 (55.8)	8.9 (9.2)	4.85 (7.1)	2.12 (3.10)

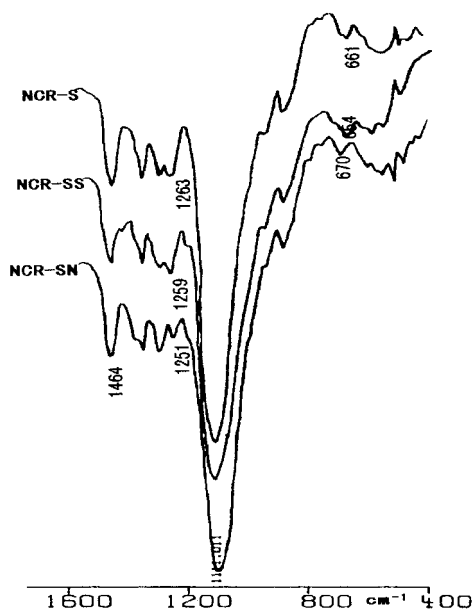


**Figure 1** IR of NCR-S, NCR-SS, and NCR-SN.

respectively. It also showed that the thermal decomposition temperature of the three resins was almost the same. The light differential was caused by the variance of the kind and content of pendent functional groups. For example, the contents of pendent functional groups in the NCR-S and NCR-SN resins are almost the same; the temperatures of the weight loss, 50 and 80%, of the NCR-S and NCR-SN resins are almost equal. However, the temperature of the 10% weight loss of the NCR-SN resin is lower (about 30°C) than that of the NCR-S resin. This indicates that the strength of C—N was lower than was the strength of C—S and the thermal stability of the pendent functional groups was lower than that of the network unit. The temperature of the weight loss of 50 and 80% of NCR-SS is the lowest among the three resins. This can be related to its having the highest content of pendent functional group among the three copolymers.

The DSC curves of NCR-SN [Fig. 2(c)] showed three separated endothermal processes at 302.9, 396.6, and 431.5°C, respectively, but, however, there were only two separated endothermal processes for NCR-S [Fig. 2(a)] and NCR-SS [Fig. 2(b)] at 387.1, 432.8°C and 396.0, 427.5°C, respectively. The two endothermal processes for the three resins were similar between 387 and 433°C. They were mainly the thermal decomposition of the network unit and the pendent functional groups. It also showed that the endothermal process at 302°C can be due to the decomposition of

pendent diethyleneamine groups in the NCR-SN resin.

### Adsorption Behavior of Resins for Metal Ions

The adsorption capacity of the NCR-S, NCR-SS, and NCR-SN resins for divalent magnesium, cobalt, copper, lead, and mercury ions was determined. The experimental results are plotted in Figure 3. It shows that the three network crown ether resins have a poor adsorption ability toward alkali-earth metal ion such as Mg(II); the adsorption ability for divalent copper, lead ions, and transition-metal ion such as Co(II) are higher than that for Mg(II). The adsorption capacity for the divalent mercury ion is the highest among all these metal ions. This can be attributed to the contribution of the bigger network crown ether cavity and the nitrogen and sulfur atoms in the pendent functional group. Sulfur and nitrogen atoms have a better binding capacity than that of the oxygen atom for Cu(II), Pb(II), Co(II), and Hg(II).

It was interesting to find that the NCR-SS and NCR-SN resins containing double coordinate atoms (S, S or S, N) have a higher adsorption capacity than that of the NCR-S resin containing monocoordinate atoms (S) in the pendent functional group. This implies that the double atomic ligands have a stronger coordination ability than that of the monoatomic ligand. The content of pendent functional groups in the NCR-SS resin is the highest among the three resins, but then its adsorption capacity is lower than that of NCR-SN. This can be related to the spatial effect of a ligand group and the coordination ability of a ligand atom.

### Adsorption Behavior of Resins for Divalent Mercury Ion

#### Effect of Temperature

In the temperature range of 20–50°C, the adsorption capacity of the three resins for the divalent mercury ion was determined:  $1/T$  versus  $\lg D$  ( $D$ : distribution ratio,  $D = Q/C_e$ ) is plotted in Figure 4. The results indicate that the distribution ratio increased with increase of the solution temperature. This shows that the adsorption process is an endothermal process and a chemical adsorption process. It also can be caused by the enhancement of the swelling ability of the resins and the ionic diffusivity in an aqueous solution with increase of the solution temperature.<sup>15</sup> For the NCR-SN

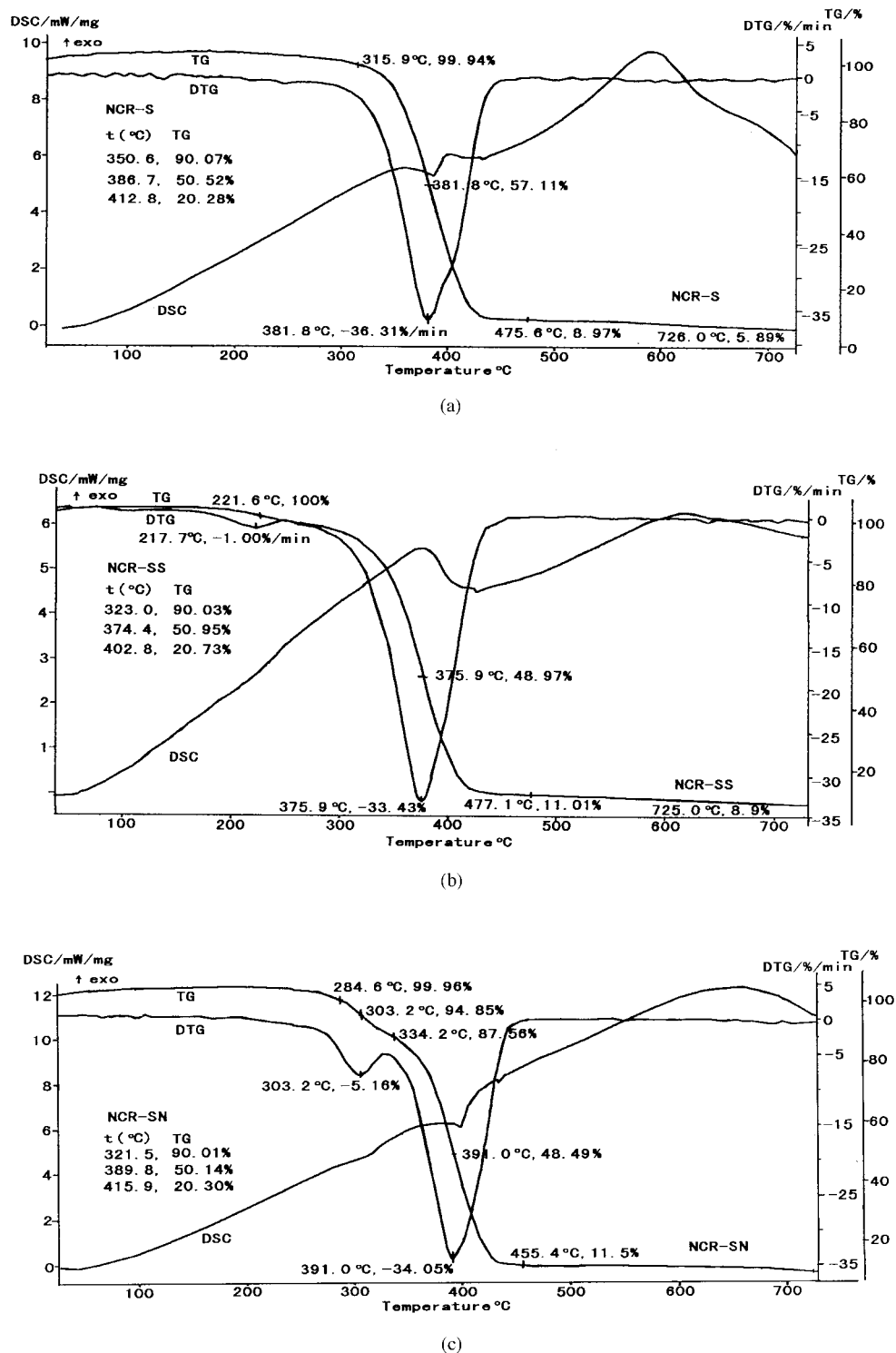


**Figure 2** TG and DSC of (a) NCR-S, (b) NCR-SS, and (c) NCR-SN.

resin, the effect of temperature on the adsorption ability is stronger than that for the NCR-S and NCR-SS resins.

In Figure 4, for NCR-S, NCR-SS, and NCR-SN, the linear slope is  $-0.450 \times 10^3$ ,  $-1.499 \times 10^3$ , and  $-3.427 \times 10^3$ , respectively; the corre-

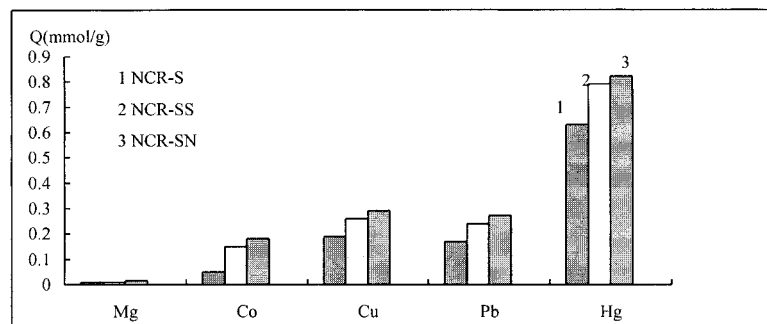


**Figure 3** Adsorption capacity of the resins (30°C, 2 h,  $C_i$  2 mmol/L).

lation coefficient ( $r$ ) is 0.995, 0.995, and 0.992, respectively. According to  $\lg D = -\Delta H/2.303RT + C$ ,  $H$  can be found for NCR-S, NCR-SS and NCR-SN as follows:  $H$  equals 8.61, 28.7, and 65.61 kJ/mol, respectively.

#### Effect of Initial pH Value of Solution

The adsorption capacity of the three resins for the divalent mercury ion was determined by using metal-ion solutions at different initial pH values (1.0–4.0). The result is shown in Figure 5. It is obvious that the higher the initial pH value is the larger the adsorption capacity is, especially for the NCR-SN resin. This can be due to protonation of the nitrogen atom in the NCR-SN resin, especially in the low initial pH value. However, no remarkable difference of the adsorption capacity was observed for the NCR-SN resin at about pH 3.5. This is also true of the other resins. The higher initial pH value can cause hydrolysis of Hg(II). So, in all the other experiments, the initial pH 3.5 of the mercury-ion solution was selected.

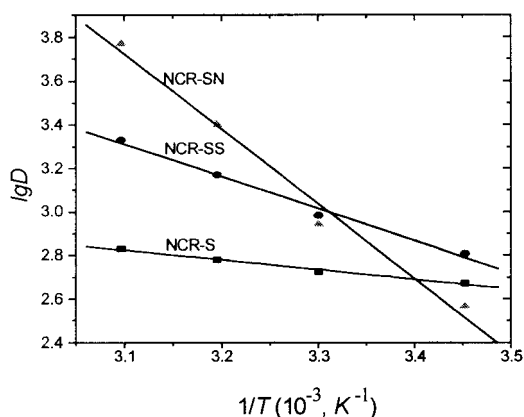


**Figure 4** Effect of temperature for the distribution ratio (pH 3.5, 2 h,  $C_i$  4 mmol/L).

#### Adsorption Rate for Hg(II)

Using a constant concentration of mercury ions (4 mmol/L) and resins (2 g/L), the concentration of the mercury ion in solution was determined at regular times. The experimental data obtained are shown in Figure 6. It shows that the three resins have a high initial adsorption rate, but the equilibrium adsorption capacity of the NCR-SN resin is larger than that of the NCR-SS resin; in turn, the equilibrium adsorption capacity of the NCR-SS resin is higher than that of the NCR-S resin. This can be because the pendent functional group of the NCR-S resin contains only one coordinate sulfur atom. The adsorption equilibrium of the three resins for Hg(II) was reached in almost 1 h.

#### Adsorption Isotherms

Using the constant concentration of the mercury ion ( $C_i$  4 mmol/L) and the changing concentration ( $CR$ ) of the resin from 1.0 to 4.0 g/L, the concentration of the mercury ion in the solution was

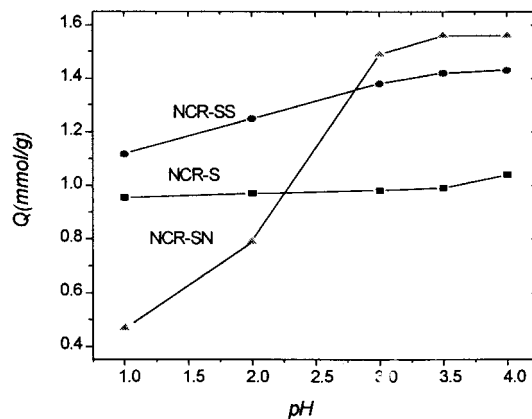


**Figure 5** Effect of initial pH value (40°C, 2 h,  $C_i$  4 mmol/L).

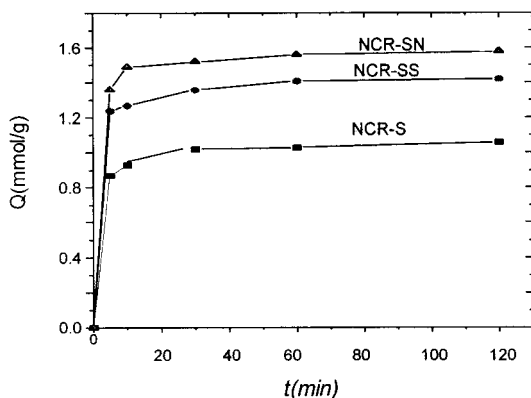


**Figure 6** Adsorption rate of three resins for Hg(II).

determined at the equilibrium adsorption. The results are shown in Figure 7(a). It is obvious that the lower concentration of the resin has the higher adsorption capacity.

The plot of  $\lg C_e$  versus  $\lg Q_e$  is shown in Figure 7(b). It is obvious that the isotherm adsorption lines fit the Freundlich model.<sup>16</sup> In the Freundlich isothermal equation,  $Q_e = K_F C_e^{1/n}$

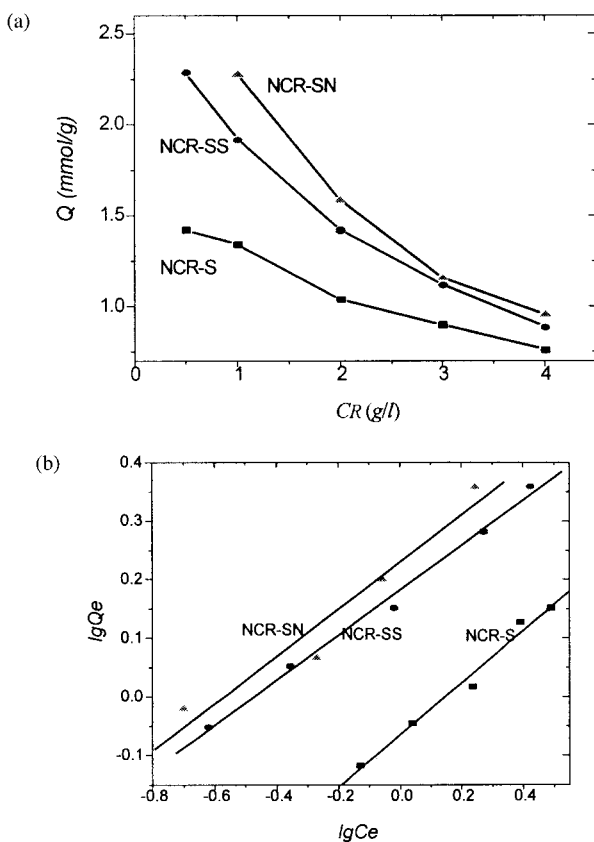


**Figure 7** (a) Effect of resin concentration; (b) linearized Freundlich isotherm.

**Table III** Langmuir and Freundlich Equation Parameters for the Best Fit and Corresponding Correlation Coefficients ( $r$ )

Resin	Freundlich Model		
	$K_F$	$1/n$	$r$
NCR-S	0.862	0.445	0.992
NCR-SS	1.535	0.384	0.996
NCR-SN	1.700	0.403	0.970
Resin	Langmuir Model		
	$K_L$	$\alpha$	$r$
NCR-S	2.107	1.299	0.998
NCR-SS	4.039	1.912	0.997
NCR-SN	6.386	3.141	0.997

and its rearrangement model  $\lg Q_e = \lg K_F + 1/n \lg C_e$ ; the Freundlich constants ( $K_F$ ,  $1/n$ ) and the corresponding correlation coefficients ( $r$ ) obtained by Figure 8(b) are listed in Table III.

From Table III, the empirical Freundlich equations for NCR-S, NCR-SS, and NCR-SN are given, respectively, as follows:  $Q_e = 0.862 C_e^{0.445}$ ,  $Q_e = 1.535 C_e^{0.384}$ , and  $Q_e = 1.70 C_e^{0.403}$ . The  $n$  values shown in Table III are between 2 to 3 for the three resins. It shows that the adsorption reactions of the three resins for the divalent mercury ion are easily and spontaneously performed.<sup>17</sup>

#### Effect of Initial Hg(II) Concentration

The adsorption capacity of the three resins for Hg(II) were determined by using different initial concentrations ( $C_i$ ) of the divalent mercury solution. The results are shown in Figure 8(a).

Figure 8(a) indicates that the adsorption capacity increased five to six times when the  $C_i$  value was increased from 0.5 to 4.0 mmol/L. When the  $C_i$  value used was over 4.0 mmol/L, the increase of the adsorption capacity was somewhat smaller. When  $C_i$  equaled 0.5 mmol/L, the removal ratio percent of NCR-S, NCR-SS, and NCR-SN for Hg(II) reached 89.1, 90.6, and 95.8%, respectively. When the initial concentration equaled 8 mmol/L, the adsorption capacity reached 285, 373, and 377 mg/g for NCR-S, NCR-SS, and NCR-SN, respectively. According to the Langmuir equation  $Q_e = K_L C_e / (1 + \alpha C_e)$  and its rearrangement model  $C_e / Q_e = (1/K_L) + (\alpha / K_L) C_e$ <sup>18</sup>,  $C_e / Q_e$  versus  $C_e$  are plotted in Figure 8(b).

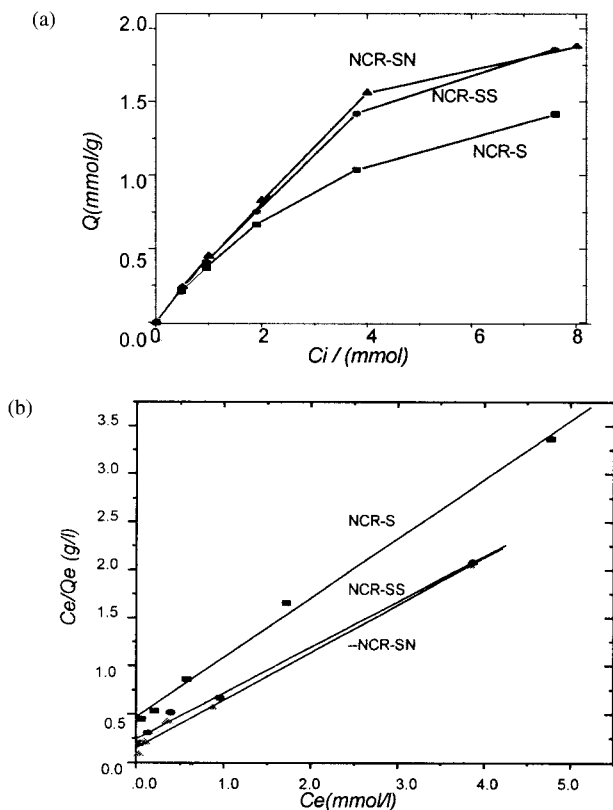


**Figure 8** (a) Effect of initial Hg(II) concentration; (b) linearized Langmuir isotherm (40°C, 2 h).

In the equation,  $K_L$  and  $\alpha$  are Langmuir constants for a given adsorbate–adsorbent system. Figure 8(b) indicates that the adsorption isotherm lines of the three resins for the divalent mercury ion are a good fit with the Langmuir model in the experimental conditions. Langmuir constants ( $K_L$ ,  $\alpha$ ) and the corresponding correlation coefficients ( $r$ ) obtained by Figure 8(b) are listed in Table III. The empirical Langmuir equations for NCR–S, NCR–SS, and NCR–SN are deduced from the data in Table III, respectively, as follows:  $Q_e = 2.107C_e/(1 + 1.299C_e)$  for NCR–S;  $Q_e = 4.036C_e/(1 + 1.912C_e)$  for NCR–SS; and  $Q_e = 6.386C_e/(1 + 3.141C_e)$  for NCR–SN.

### X-ray Photoelectron Spectroscopy

The adsorption mechanism of the NCR–SN resin for Cu(II), Pb(II), and Hg(II) was investigated using X-ray photoelectron spectroscopy. O1s binding energies of the complexes (L–M) of the NCR–SN ligand (L) with metal ions are almost the same as that of the NCR–SN ligand. The N1s binding energies of L–Cu(II), L–Pb(II), and

L–Hg(II) are 0.55, 0.50, and 0.32 eV higher than that of NCR–SN, respectively. The S2p binding energies of L–Cu(II), L–Pb(II), and L–Hg(II) are 0.90, 0.82, and 0.59 eV higher than that of NCR–SN, respectively. The Cu2p, Pb4f, and Hg4f binding energies of L–Cu(II), L–Pb(II), and L–Hg(II) are 2.13, 2.01, and 0.80 eV lower than that of the corresponding M(II), respectively. It indicates that the adsorption of the NCR–SN resin toward Cu(II), Pb(II), and Hg(II) is accomplished mainly by the chemical coordination of the ligand atom (S, N) of the pendent functional groups with the metal ions.

### CONCLUSIONS

Network crown ether resins with a high content of pendent functional groups were prepared and characterized by IR, elemental analysis, and thermal analysis. The slight variance of the thermal stability of the resins is related to the kind and content of the pendent functional groups. The adsorption capacity of the resins for Hg(II) is higher than that for Cu(II), Co(II), and Pb(II). The adsorption of the resins for Hg(II) is easy and spontaneously performed. The adsorption of the NCR–SN resin toward Cu(II), Pb(II), and Hg(II) is accomplished mainly by the chemical coordination of the ligand (S, N) of the pendent functional groups with the metal ions.

The authors thank the National Nature Science Foundation of China for financial assistance. We also thank Mr. H. Zhou of the Coal Combustion Laboratory, Center China University of Technology, for his assistance in the thermal analysis experiments.

### REFERENCES

1. Kvan, T. C.; Chiou, C. L.; Wang, S. J. *Polym Bull (Berl)* 1983, 9, 216.
2. Wong, L. H.; Smid, J. *J Am Chem Soc* 1977, 99, 5637.
3. Diamali, M.; G. Burba, P.; Lieser, K. H. *Angew Makromol Chem* 1980, 92, 145.
4. He, Y. B.; Meng, L. Z.; Chen, F. J.; Wu, C. T. *Ion Exch Adsorp* 1998, 14, 261 (in Chinese).
5. Warshawsky, A.; Kalir, R.; Deshe, A.; Berkovitz, H.; Patchornik, A. *J Am Chem Soc* 1997, 101, 4249.
6. Gao, F.; Xu, Y. W. *J Appl Polym Sci* 1997, 65, 931.
7. Chen, Y. Y.; Feng, M. H. *J Appl. Chem* 1986, 7, 651 (in Chinese).



8. Chen, Y. Y.; Lu, X. R.; Cai, M. Z.; Song, X. P. *Funct Polym* 1990, 3, 122 (in Chinese).
9. Dietzmann, I.; Tomanova, D.; Metflejs, J. *Collect Czech Chem Commun* 1974, 39, 123.
10. Fong, H. O.; Hardstaff, W. R.; Kay, D. G.; Langler, R. F.; Morse, R. H.; Sandoval, D. N. *Can J Chem* 1979, 57, 1206.
11. Booth, E.; Burnop, V. C. E.; Jones, W. E. *J Chem Soc* 1944, 666.
12. Chinton, R. O.; Suter, C. M.; Laskowski, S. C.; Jackmen, M.; Huber, W. *J Am Chem Soc* 1945, 67, 594.
13. He, Y. B.; Meng, L. Z.; Wu, C. T.; Qian, T. *J Appl Polym Sci* 1999, 74, 1278.
14. Mitra, B. C.; Basak, R. K.; Sarkar, M. *J Appl Polym Sci* 1998, 67, 1093.
15. Huang, W. Q.; Si, Z. H.; Li, C. X.; He, B. L. *Ion Exch Adsorp* 1997, 13, 307 (in Chinese).
16. Juang, R. S.; Tseng, R. L.; Wu, F. C.; Lee, S. H. *J Chem Tech Biotechnol* 1997, 70, 391.
17. Lafuma, F.; Audebert, R.; Quivoron, C. Y. P. *Inorg Chim Acta* 1982, 66, 167.
18. Ahmad, A. H. A.; Ribhi, E. B. *J Chem Tech Biotechnol* 1997, 69, 27.